ACS ENVIRONMENTAL Au
AN OPEN ACCESS JOURNAL OF THE AMERICAN CHEMICAL SOCIETY

pubs.acs.org/environau
Article

Plasmid Backbone Impacts Conjugation Rate, Transconjugant Fitness, and Community Assembly of Genetically Bioaugmented Soil Microbes for PAH Bioremediation

Published as part of ACS Environmental Au special issue "2024 Rising Stars in Environmental Research".

Tessa M. Crosby and Lauren B. Stadler*

Cite This: *ACS Environ. Au* 2025, 5, 241−252

Read Online

ACCESS | Metrics & More | Article Recommendations | Supporting Information

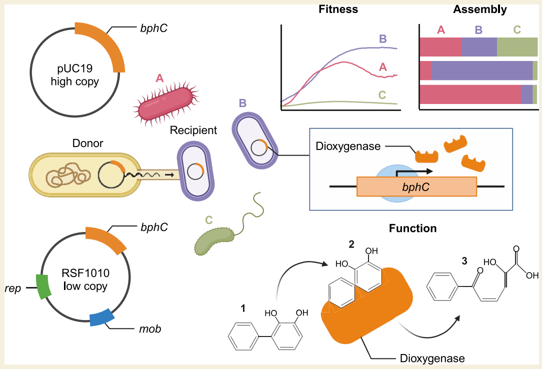

ABSTRACT: Many polycyclic aromatic hydrocarbons (PAHs) in the environment resulting from crude oil spills and the incomplete combustion of organic matter are highly toxic, mutagenic, or carcinogenic to microorganisms and humans. Bioremediation of PAHs using microorganisms that encode biodegradative genes is a promising approach for environmental PAH cleanup. However, the viability of exogenous microorganisms is often limited due to competition with the native microbial community. Instead of relying on the survival of one or a few species of bacteria, genetic bioaugmentation harnesses conjugative plasmids that spread functional genes to native microbes. In this study, two plasmid backbones that differ in copy number regulation, replication, and mobilization genes were engineered to contain a PAH dioxygenase gene (*bphC*) and conjugated to soil bacteria including *Bacillus subtilis*, *Pseudomonas putida*, and *Acinetobacter* sp., as well as a synthetic community assembled from these bacteria. Fitness effects of the plasmids in transconjugants significantly impacted the rates of conjugative transfer and biotransformation rates of a model PAH (2,3-dihydroxybiphenyl). A synergistic effect was observed in which synthetic communities bioaugmented with *bphC* had significantly higher PAH degradation rates than bacteria grown in monocultures. Finally, conjugation rates were significantly associated with the relative abundances of bacteria in synthetic communities, underscoring how fitness impacts of plasmids can shape the microbial community structure and function.

KEYWORDS: *genetic bioaugmentation, conjugation, polycyclic aromatic hydrocarbons, bioremediation, dioxygenase*

■ INTRODUCTION

The environmental dispersal of PAHs from the burning of fossil fuels has greatly expanded their structural variation, making them the broadest range of nonhalogenated pollutants in our biosphere.[1,2] These hydrophobic pollutants concentrate in the lipids of exposed wildlife and bioaccumulate in the food chain,[2] causing premature death[3,4] and cancer.[5,6] Between 1907 and 2014, approximately 7 million tons of oil leaked into coastal environments from over 140 spills,[7] causing immense damage to marine ecosystems.[8,9] In addition to being mutagenic, persistent, and bioaccumulative, PAHs can negatively impact soil bacteria,[10,11] resulting in reduced cell membrane integrity[12] and oxygen exchange,[13] altered microbial diversity,[14] and decreased cycling of vital nutrients like nitrogen.[15] Soil microbes can evolve biodegradative enzymes over time when exposed to PAHs in the environment; however, this process occurs very slowly.[16]

To clean up PAH spills, microorganisms with catabolic genes capable of PAH biotransformation have been introduced into contaminated soil environments to expedite PAH removal in a process called *in situ* bioremediation.[17−19] While successful examples of PAH bioremediation exist,[20−23] studies often report an initial increase in bacterial seed populations immediately after addition to contaminated soil, followed by a decrease in abundance over time.[24,25] This was likely due to competition between exogenous microorganisms and the indigenous microbial community. Exogenous bacteria are especially vulnerable to being outcompeted by environmental microbes because they may not be well adapted to site-specific nutrient availability. Additionally, the survival of inoculated bacteria is unpredictable in soil environments due to dynamic

Received: November 5, 2024
Revised: January 9, 2025
Accepted: January 13, 2025
Published: January 22, 2025

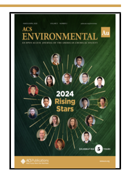

https://doi.org/10.1021/acsenvironau.4c00123
ACS Environ. Au 2025, 5, 241−252

physical, biological, and chemical factors that shape the microbial ecology.

Genetic bioaugmentation is an approach that focuses on the delivery of functional genes via mobile genetic elements such as plasmids rather than bacteria for contaminant removal. Plasmids harboring biodegradative genes are widely shared among bacteria in many environments, including soil,[26−28] groundwater,[29] and wastewater.[30] Additionally, plasmids play a critical role in bacterial ecology and evolution, as they are capable of spreading biodegradative functions across phylogenetic barriers and serve as vehicles for novel metabolic gene expressions *in situ*.[28,31−33] The premise of genetic bioaugmentation is that plasmid DNA can be harnessed to spread biodegradative genes to recipient bacteria, known as transconjugants, in bacterial communities. Distributing biodegradative genes across numerous bacterial species may improve bioremediation rates and longevity, as a greater diversity of engineered organisms will not be as easily outcompeted by native bacteria. Although previous studies have used catabolic plasmids for bioaugmentation,[28,34,35] little is known about how plasmid selection impacts conjugation and biotransformation rates in soil microorganisms and microbial communities.

Plasmid backbones pUC19 and RSF1010 are great candidates for differentiating plasmid-specific characteristics that may influence the efficiency of genetic bioaugmentation because they differ in key factors known to affect the plasmid conjugation rate and the transcription of recombinant DNA. These factors include host range, copy number regulation, mode of replication, and mobilization genes. RSF1010 plasmid codes for its own replication and mobilization initiation genes and regulates its own copy number to reduce negative fitness impacts often associated with maintaining plasmid DNA.[36,37] Due to the independent mode of plasmid maintenance and minimal fitness impacts afforded by RSF1010, it is thought to have a broad host range.[38] In contrast, pUC19 is a high-copy-number plasmid[39] that must rely on host-encoded proteins for stable DNA replication and maintenance. Maintaining high-copy-number plasmids often redirects host-encoded DNA replication and transcription proteins away from growth-promoting pathways, and therefore, pUC19 is thought to impose a significant growth burden on host cells.[40−42] Despite its narrow host range, the pUC19 cloning plasmid allows researchers to rapidly produce high titers of recombinant bioremediation proteins due to its copy number. To observe how fitness determinants of pUC19 and RSF1010 impact downstream conjugation and bioremediation rates, both plasmids were used in this study to deliver a bioremediation gene to multiple species of bacteria.

In aerobic environments, the catabolism of PAHs is often initiated by hydroxylation, which is catalyzed by oxygenase enzymes.[43−45] Catabolic *bph* genes, such as *bphC*, have been isolated from soil bacteria[46,47] and shown to catalyze the meta-ring cleavage of many hydroxylated PAHs, including dibenzofuran, naphthalene, and catechol.[48] Biodegradative gene *bphC* codes for 2,3-dihydroxybiphenyl 1,2-dioxygenase (2,3-DBDO), the third enzyme in the PCB catabolic pathway.[49] The ring-cleavage activity afforded by 2,3-DBDO is thought to be the rate-limiting step in initiating the degradation of halogenated aromatic hydrocarbons because it is responsible for opening cyclic compounds that are further degraded in downstream metabolic pathways.[50] Additionally, 2,3-DBDO has a wide substrate specificity and can readily cleave halogenated aromatics at the distal position, avoiding the formation of a strong enzyme inhibitor.[51] Thus, the *bphC* gene can be harnessed to improve the efficiency of PAH biodegradation by overcoming bottlenecks in the degradation process and limiting the effects of enzyme inhibition. Two prior studies used 2,3-DBDO encoded on nonmobilizable plasmids for bioremediation,[52,53] but none to our knowledge have mobilized *bphC* to soil bacteria using conjugative plasmids. To advance the genetic bioaugmentation of PAHs using conjugative plasmids, a better understanding of transfer rates of conjugative plasmids to soil microorganisms, their fitness impacts on recipient microorganisms, and how they impact overall rates of PAH biodegradation is needed.

Genetic bioaugmentation of biodegradative genes depends on numerous factors, including conjugation rates of plasmids, host range of plasmids, fitness impacts of plasmids in transconjugant bacteria, and the transcription and translation of biodegradative genes and enzymes in transconjugant bacteria. In this study, we engineered two different plasmids, pUC19 and RSF1010, which contain the *bphC* gene. We then measured the conjugation rates of our engineered plasmids and fitness impacts of the plasmids on three model soil bacteria, as well as a mixture of these bacteria. Furthermore, we investigated if there was an association between conjugation rates and relative abundances of soil bacteria in engineered synthetic communities. Finally, we recorded the biotransformation rates of a model PAH (2,3-dihydroxybiphenyl) by soil transconjugants engineered with *bphC* plasmids and compared these rates to nonengineered controls.

MATERIALS AND METHODS

Plasmid and Donor Construction

We added the *bphC* gene to two different plasmid backbones, pUC19 and RSF1010, to create plasmids pUC19-bphC (GenBank accession no. PQ159146) and pRSF1010-bphC (GenBank accession no. PQ159147). Plasmid backbones and DNA inserts for pUC19-bphC and pRSF1010-bphC construction were amplified using Q5 High-Fidelity 2× Master Mix (NEB). Descriptions of the plasmids used in this study can be found in Table S1, and cycling conditions and primer sequences used to amplify DNA inserts for plasmid construction can be found in Table S2. After the amplification of DNA parts, *bphC* plasmids were assembled using the NEBridge BsaI-HFv2 Golden Gate Assembly Kit (NEB). A figure demonstrating plasmid maps for our assembled pUC19-bphC and pRSF1010-bphC constructs can be found in Figure S1.

After golden gate assembly, *bphC* plasmids were transformed into competent NEB Turbo (NEB) following the manufacturer's electroporation protocol. Next, NEB Turbo bacteria were plated on LB agar supplemented with 25 μg/mL streptomycin to select for cells that successfully replicated pUC19-bphC or pRSF1010-bphC assemblies. A single CFU was inoculated the following day in an LB medium supplemented with streptomycin and grown overnight at 37 °C while being shaken at 225 rpm. Plasmid DNA was then extracted and purified using the QIAprep Spin Miniprep Kit (Qiagen) and sent to Plasmidsaurus for whole plasmid sequencing using Oxford Nanopore Technology with custom analysis and annotation. Sequence-confirmed pUC19-bphC and pRSF1010-bphC plasmids were electroporated into competent MFDpir *Escherichia coli*, an auxotrophic strain that requires diaminopimelic acid (DAP) in media for growth.[54] Using a DAP-dependent donor allows for an easy counterselection against MFDpir after conjugation. Cells were recovered using SOC recovery media +0.3 mM DAP. Finally, MFDpir bacteria were plated on an LB agar supplemented with 25 μg/mL streptomycin and 0.3 mM DAP to select for plasmid donors that successfully replicated pUC19-bphC or pRSF1010-bphC.

https://doi.org/10.1021/acsenvironau.4c00123
ACS Environ. Au 2025, 5, 241−252

Bacterial Conjugation and Growth Assay

To account for donor, recipient, and transconjugant growth effects in conjugation frequency calculations, maximum growth rates (h^{-1}) of these bacteria were included in an adapted Simonsen method.[55] Here, we assessed the fitness of each group (donor, recipients, and transconjugants) by comparing their maximum growth rates.[56,57] Bacterial strains used in this study can be found in Table S3. A single CFU of *B. subtilis*, *P. putida*, and *Acinetobacter* sp. were inoculated in LB media without antibiotics or DAP, and single CFUs of MFDpir donors were inoculated in LB media supplemented with 25 μg/mL streptomycin and 0.3 mM DAP. Bacteria were then grown overnight at 35 °C, shaking at 225 rpm. The following day, cultures were diluted 1:100, allowed to reach early exponential growth phase (Figure S2), and washed with 1× phosphate buffer saline (PBS) to remove spent media. Then, cultures were diluted 1:100 in DAP medium without antibiotics to support the growth of DAP-dependent MFDpir donors and antibiotic-sensitive recipients during conjugation. Immediately, diluted cultures were plated in serial dilution on their respective agar types to count initial populations in CFU/mL. Negative control plates in which MFDpir donors were plated on LB agar without DAP and recipients on streptomycin were also prepared.

To assemble conjugation mixtures, bacteria were mixed in a 1:1 volumetric mixture of 50 μL of donor to 50 μL of recipient in triplicate. To assemble conjugation mixtures with synthetic communities, an equivalent volume of each previously diluted recipient was mixed and then added in a 1:1 volumetric ratio of 50 μL of donor to 50 μL of synthetic community bacteria in triplicate. In addition to assembling conjugation mixtures with diluted cells, 50 μL of donor, recipient, or synthetic community was added to 50 μL of DAP media in triplicate. These diluted monocultures served as negative conjugation controls and were included alongside conjugation experiments to measure donor and recipient growth rate(s) for conjugation rate calculations. Triplicates were incubated at 35 °C for 6 h under static conditions to promote bacterial conjugation, and 600 nm absorbance measurements were taken every 10 min using a Tecan Spark Multimode Microplate Reader to account for monoculture growth in conjugation frequency calculations. Absorbance values recorded at 600 nm were normalized to blank DAP media (Figure S2).

After conjugation experiments were complete, triplicates were washed with 1× PBS to remove DAP media and plated in serial dilution on the following: (1) LB + streptomycin agar without DAP to count transconjugants, (2) LB + streptomycin with 0.3 mM DAP to count donors + transconjugants, and (3) LB without antibiotics or DAP to count recipients + transconjugants. End-point population counts in CFU/mL of donors were calculated by subtracting plate (1) from plate (2), recipients were calculated by subtracting plate (1) from plate (3), and transconjugants were simply counted from DAP without antibiotic plates (1). Negative control conditions (monocultures) did not grow on the LB + streptomycin agar without DAP, meaning no transconjugants were observed.

Absorbance data collected during the 6 h conjugation period was processed using the growth rates package[58] in R to determine maximum growth rates (h^{-1}) from the exponential growth phase. Conjugation frequencies that incorporated the maximum growth rates determined in R were calculated using an adapted Simonsen method.[55] Figures depicting conjugation and maximum growth rate (h^{-1}) data were constructed by using BioRender. Finally, a Tukey test ($p < 0.05$) was performed after a two-way ANOVA analysis ($p < 0.05$) in R to determine the statistical significance of (1) conjugation rates between plasmids and across recipients and (2) maximum growth rates between engineered (containing a plasmid) and nonengineered bacteria (no plasmid). Prior to performing a two-way ANOVA statistical test, conjugation and growth rate data were (1) fit to a linear model ($p < 0.05$) to check if residuals were normally distributed and (2) analyzed using the F test ($p > 0.05$) to assess variance.

Determining Relative Abundances of Bacteria from Synthetic Communities

To investigate how fitness impacts of plasmids in transconjugants affect synthetic community assembly, DNA was extracted and 16S rRNA gene amplicon sequencing was performed on synthetic communities immediately before and after conjugation experiments. Here, the relative abundances of bacteria in synthetic communities reflect bacterial fitness because they indicate the ability of the bacteria to grow and reproduce within consortia and in direct competition with surrounding microbes.[57,59,60] Furthermore, the relative abundances of bacteria in engineered synthetic communities were compared to nonengineered communities to demonstrate how community structures shift to favor the growth of the most fit transconjugants.

For determining the relative abundance profiles of synthetic communities before conjugation, approximately 100 μL of synthetic communities assembled from recipients grown to the early exponential phase (prior to conjugation mixture assembly) were plated on LB agar and allowed to incubate overnight at 35 °C. After end-point population counts were recorded following the 6 h conjugation period, the remaining volume (∼100 μL) of PBS-washed conjugation mixtures with synthetic communities was plated on the transconjugant-selective LB agar (streptomycin without DAP to exclude MFDpir donors) and allowed to incubate overnight at 35 °C. Negative control monocultures (∼100 μL) were also plated on their appropriate agar type after the 6 h conjugation experiment to extract reference 16S DNA. The next day, all bacteria were scraped from plates into 100 μL 1× PBS and lysed to extract total DNA using the Maxwell RSC PureFood GMO and Authentication Kit (Promega). DNA extracts were then subjected to PCR amplification of the variable V3−V4 region of the 16S rRNA gene with Illumina adapters. Primer sequences and PCR cycling conditions used to amplify 16S rRNA genes can be found in Table S2. Purified amplicons from monocultures were sent for Sanger sequencing (Azenta Life Sciences), while synthetic community amplicons were sent for next-generation sequencing using the MiSeq 2× 250 bp Illumina configuration. Sequencing statistics for synthetic community samples can be found in Table S4.

To process raw sequencing data, paired end sequences were imported into QIIME2[61,62] for demultiplexing and denoising using the demux[63] and dada2[64] plugins to yield a count table of amplicon sequence variants (ASVs). ASVs were removed from the total reads if they reported sequences of less than 0.1% of the average variant reads per sample. Then, the remaining ASVs were filtered by removing sequences that shared less than 98% identity with the reference 16S rRNA genes of the sequenced DNA from bacteria used in this study. Taxonomic classifications of the remaining ASVs were assigned using custom BLAST searches from the National Center for Biotechnology Information (NCBI) web site. These custom searches were performed using the Nucleotide collection database with highly similar sequences (megablast). Filtered ASVs and their BLAST IDs can be found in Table S5. Finally, a one-way ANOVA test ($p < 0.05$) was performed in R to determine statistical significance between the relative abundance profiles of nonengineered synthetic communities, synthetic communities engineered with pUC19-bphC, and synthetic communities engineered with pRSF1010-bphC. Prior to performing a one-way ANOVA statistical test, relative abundance data were (1) fit to a linear model ($p < 0.05$) to check if residuals were normally distributed and (2) analyzed using the F test ($p > 0.05$) to assess variance. To observe whether there was a direct relationship between the conjugation rate and synthetic community assembly, a Spearman rank correlation test was performed between conjugation rates and relative abundance values in R.

Dioxygenase Functional Assay

To compare dioxygenase activities of engineered bacteria with their nonengineered counterparts, an absorbance-based protocol was adapted from Furukawa and Miyazaki.[65] To determine the dioxygenase activities of nonengineered recipients, approximately 100 μL of *B. subtilis*, *P. putida*, and *Acinetobacter* sp. grown to the early

https://doi.org/10.1021/acsenvironau.4c00123
ACS Environ. Au 2025, 5, 241−252

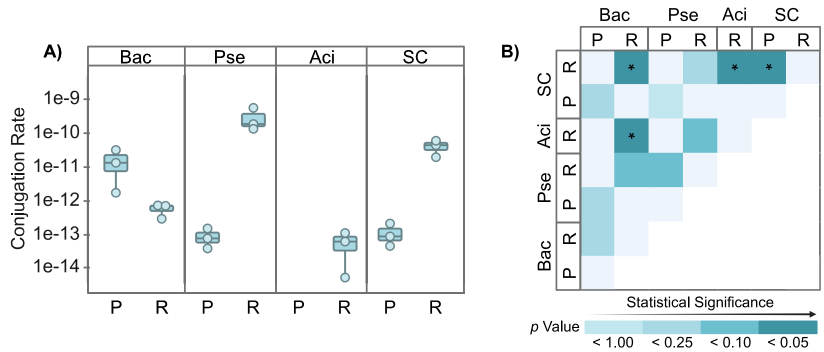

Figure 1. (A) Conjugation rates determined from different recipient and plasmid combinations and a (B) heatmap showing p values based on a two-way ANOVA statistical analysis followed by a Tukey test from pairwise comparisons of conjugation rates. p values below 0.05 are denoted as significant with an asterisk (*). Triplicate measurements are shown as dots, horizontal lines indicate the mean, and box plots indicate the standard deviation. Recipients include Bac, *B. subtilis*; Pse, *P. putida*; Aci, *Acinetobacter* sp.; and SC, synthetic community. Bacteria engineered with plasmids pUC19-bphC and pRSF1010-bphC are denoted as "P" and "R", respectively.

exponential phase were plated on LB agar and allowed to incubate overnight at 35 °C. Nonengineered synthetic communities were assembled the following day from equivalent volumetric fractions of these bacteria resuspended in 1× PBS. To determine the dioxygenase activities of engineered transconjugants, approximately 100 μL of PBS-washed conjugation mixtures was plated on a transconjugant-selective LB agar (streptomycin without DAP to exclude MFDpir donors) and allowed to incubate overnight at 35 °C. Nonengineered recipients and transconjugants were scraped from plates into 100 μL 1× PBS and diluted 1:100 in (1) M9 minimal salts media, (2) M9 minimal salt media supplemented with 100 μM of 2,3-dihydroxybiphenyl (Millipore Sigma), or (3) M9 minimal salts media supplemented with 100 μM of 2,3-dihydroxybiphenyl and 100 μM of 3-chlorocatechol (Millipore Sigma), a strong inhibitor of the *bphC* enzyme,[66] in triplicate. As 2,3-dihydroxybiphenyl is converted to its meta-ring cleaved product, 2-hydroxy-6-oxo-6-phenylhexa-2,4, via dioxygenase activity, a colorimetric change occurs that can be observed at a 434 nm absorbance.[67] Absorbance readings were taken at 434 nm every 10 min for 24 h under static conditions at 35 °C using a Tecan Spark Multimode Microplate Reader. Absorbance measurements were also recorded at 600 nm to see whether bacteria could utilize 2,3-dihydroxybiphenyl or its cleaved byproduct to promote bacterial growth. Normalized 434 nm absorbance data can be found in Figure S3, and normalized 600 nm absorbance data can be found in Figure S4. There was no observed change in either absorbance assay for bacteria suspended in M9 minimal media or M9 minimal media with both 100 μM 2,3-dihydroxybiphenyl and 3-chlorocatechol, confirming that any change in absorbance for bacteria in M9 minimal media with 100 μM 2,3-dihydroxybiphenyl was due to the dioxygenase activity. Absorbance readings were first normalized to their appropriate blank media control, followed by analysis using the growthrates package[58] in R to determine maximum biotransformation and growth rates (h^{-1}) from the exponential growth phase. Figures depicting maximum biotransformation and growth rate (h^{-1}) data were constructed by using BioRender. Finally, a Tukey test ($p < 0.05$) was performed after a two-way ANOVA analysis ($p < 0.05$) in R to determine the statistical significance of the maximum biotransformation and growth rates between engineered and nonengineered bacteria. Prior to performing a two-way ANOVA statistical test, biotransformation and growth data were (1) fit to a linear model ($p <$ 0.05) to check if residuals were normally distributed and (2) analyzed using the F test ($p > 0.05$) to assess variance.

To assess if recipient type and the bioaugmentation of *bphC* interacted with each other to significantly increase biotransformation rates, a two-way ANOVA with interaction test was used.[68−70] Finding a significant interaction between these two variables would suggest a strong dependence of the effectiveness of one variable on another. Prior to performing the two-way ANOVA with interaction analysis, the biotransformation rate data were fit to a linear model and subjected to an F test ($p > 0.05$) as described in the two-way ANOVA without interaction analysis. After these statistical tests verified that data were distributed normally and variance between groups was greater than variance within groups, we performed a two-way ANOVA with an interaction test ($p < 0.05$) on biotransformation rates between (1) nonengineered and engineered bacteria and (2) bacteria grown in monocultures versus synthetic communities.

To determine whether there was a synergistic effect observed in which PAH biotransformation rates were significantly higher in the synthetic communities as compared to the additive rates of the individual monocultures, we performed a linear contrast analysis.[71] Four species variables (*B. subtilis*, *P. putida*, *Acinetobacter* sp., and synthetic communities) with three treatments (nonengineered, engineered with pUC19-bphC, and engineered with pRSF1010-bphC) were analyzed using linear combinations of biotransformation rates. These linear combinations were used to assess whether the mean of biotransformation rates from nonengineered synthetic communities was significantly different from the additive means of biotransformation rates of nonengineered monocultures ($p < 0.05$). Contrast analyses were repeated for biotransformation rates collected from synthetic communities and monocultures engineered with pUC19-bphC and pRSF1010-bphC.

RESULTS

Conjugation Rates Varied Significantly across Recipients and between Plasmids

To understand plasmid-specific factors that drive conjugation efficiency and impact transconjugant fitness, we compared the delivery of a biodegradative gene using plasmid backbones pUC19 and RSF1010. These plasmids differ in copy number, replicative origin, and mobilization genes. We used an adapted Simonsen method[72] to calculate conjugative transfer efficiency because it accounts for the effects of donor, recipient, and transconjugant population growth.[55] Using this method, our conjugation rate measurements captured fitness effects of the bacteria involved, which are often ignored in conjugation assays. MFDpir donors containing engineered pUC19 or RSF1010 plasmids were mixed with three model soil bacteria, as well as a synthetic community consisting of a mixture of all three bacteria, to determine fitness effects of plasmids in transconjugants and whether these effects translated into a competitive community context.

We first compared the conjugation rates of pUC19 and RSF1010 plasmid backbones that were engineered to contain the *bphC* gene (Figure 1A). RSF1010 plasmid harbors its own complete replicon and plasmid maintenance genes that function independently from host-specific DNA proteins,[36,37] while the pUC19 plasmid must rely on host-encoded proteins for stable replication and copy number control. We found that pRSF1010-bphC conjugation rates were four magnitudes higher to *P. putida* and significantly higher to synthetic communities when compared to conjugation rates of pUC19-bphC (Figure 1B; $p < 0.05$). Across the three soil recipients, conjugative transfer rates of pRSF1010-bphC to *P. putida* were three and four orders of magnitude higher than to *B. subtilis* and *Acinetobacter* sp., respectively. Furthermore, the conjugation rates of pRSF1010-bphC observed from synthetic community matings were significantly higher than for *B. subtilis* and *Acinetobacter* sp. matings (Figure 1B; $p < 0.05$), but similar to those observed from *P. putida* (Figure 1B; $p > 0.10$).

We found that conjugative transfer rates of pUC19-bphC to recipients were lower than those of pRSF1010-bphC, except when *B. subtilis* was used as a recipient organism in conjugative matings. For *B. subtilis*, the conjugation rates of pUC19-bphC were two orders of magnitude higher than those of pRSF1010-bphC. Although pUC19-bphC conjugative transfer rates were not significantly different across recipients, this plasmid was delivered to *B. subtilis* at rates that were three orders of magnitude higher than of *P. putida* and SC rates. Interestingly, we observed no conjugation of pUC19-bphC to *Acinetobacter* sp. from MFDpir donor, even when conjugation experiments were extended to 24 h.

Together, these results were in agreement with the SC composition data determined using 16S rRNA gene sequencing (Figure 2). After conjugating our engineered RSF1010

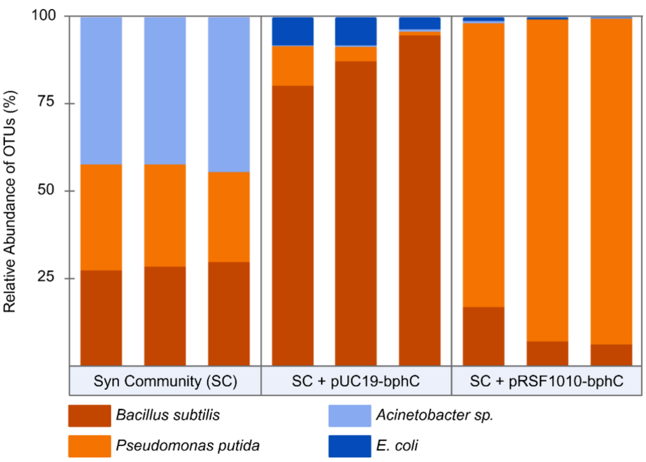

Figure 2. Relative abundance profiles of the SC members as determined by 16S rRNA gene sequencing. The left panel shows the synthetic communities (SCs) before conjugation, the middle panel shows the SCs after conjugation with pUC19-bphC, and the right panel shows the SCs after conjugation with pRSF1010-bphC.

vector to synthetic communities, *P. putida* were significantly enriched to a relative abundance of 89% ± 6.6, as compared to nonengineered communities where their relative abundance was 29% ± 2.4 ($p < 0.01$). Furthermore, *B. subtilis* and *Acinetobacter* sp. relative abundances were significantly reduced from 29% ± 1.2 to 10% ± 6.0 and 43% ± 1.2 to < 1.0%, respectively, when compared to nonengineered synthetic communities ($p < 0.01$). This is consistent with our monoculture experiments for which we observed that *P. putida* had the highest conjugation rates for pRSF1010-bphC (Figure 1A). Our conjugation results also corroborated 16S rRNA gene relative abundance data from synthetic communities engineered with the pUC19 derivative, as *B. subtilis* fractions were significantly enriched to 88% ± 7.2 ($p < 0.01$), while *P. putida* fractions were significantly reduced to 5.6% ± 5.3 ($p < 0.01$) when compared to nonengineered communities. Overall, conjugation data collected from monoculture recipients were consistent with the SC assembly results, as individual bacteria that received plasmids at the highest rates of transfer dominated synthetic communities engineered with the same plasmids.

Fitness Effects of Transconjugants Reflected in Conjugation Rates and SC Compositions

To investigate the fitness impacts of our engineered plasmids on recipient soil bacteria, we measured the maximum growth rates of nonengineered (no plasmid) and engineered (plasmid-bearing) bacteria in nutrient-rich media. We compared maximum growth rates across nonengineered organisms and engineered organisms with different plasmid backbones (Figure 3A) and observed significant differences across recipient bacteria. The maximum growth rates of nonengineered *Acinetobacter* sp. were significantly lower than nonengineered *B. subtilis* and *P. putida* rates (Figure 3B; $p < 0.01$ and $p < 0.05$, respectively). The low growth rates demonstrated from nonengineered *Acinetobacter* sp. may explain the low observed rates of pRSF1010-bphC transfer in conjugative matings (Figure 1A) when compared to other recipients, as the adapted Simonsen method accounts for recipient growth when calculating conjugative transfer rate.

The maximum growth rates of pUC19 and RSF1010 engineered transconjugants were not significantly different from each other, indicating that the fitness of our *bphC* plasmids was relatively similar for each recipient in nutrient-rich media. However, the maximum growth rates of *B. subtilis* engineered with pUC19-bphC were 91% ± 17 higher than those observed from *B. subtilis* engineered with pRSF1010-bphC. Moreover, the maximum growth rates of *B. subtilis* engineered with pRSF1010-bphC were 35% ± 58 lower than those observed from its nonengineered counterparts, indicating a negative fitness cost for maintaining the RSF1010 plasmid. Maximum growth rates of *P. putida* with and without engineered plasmids were not significantly different from one another. This is also true in the case of the *Acinetobacter* sp. and RSF1010 engineered counterparts as well as SCs and their engineered counterparts.

In addition to comparing fitness effects between the same recipient bacteria engineered with two different plasmids, we also compared maximum growth rates across different recipient bacteria to understand the fitness impacts of the same plasmid in different hosts. *P. putida* engineered with pRSF1010-bphC had maximum growth rates 77% ± 51 and 52% ± 79 higher than those observed from *B. subtilis* and *Acinetobacter* sp. engineered with pRSF1010-bphC, respectively. Likewise, SCs engineered with pRSF1010-bphC had maximum growth rates approximately 83% ± 43 and 57% ± 71 higher than those observed from *B. subtilis* and *Acinetobacter* sp. engineered with pRSF1010-bphC, respectively.

Ultimately, transconjugant fitness effects were reflected in conjugation data, as maximum growth and conjugation rates observed from pUC19-bphC engineered recipients were highest with *B. subtilis* as the recipient. Furthermore, SCs engineered with pUC19-bphC were significantly enriched with *B. subtilis*. In the case of pRSF1010-bphC engineered organisms, the maximum growth rates of *P. putida* and SC

https://doi.org/10.1021/acsenvironau.4c00123
ACS Environ. Au 2025, 5, 241−252

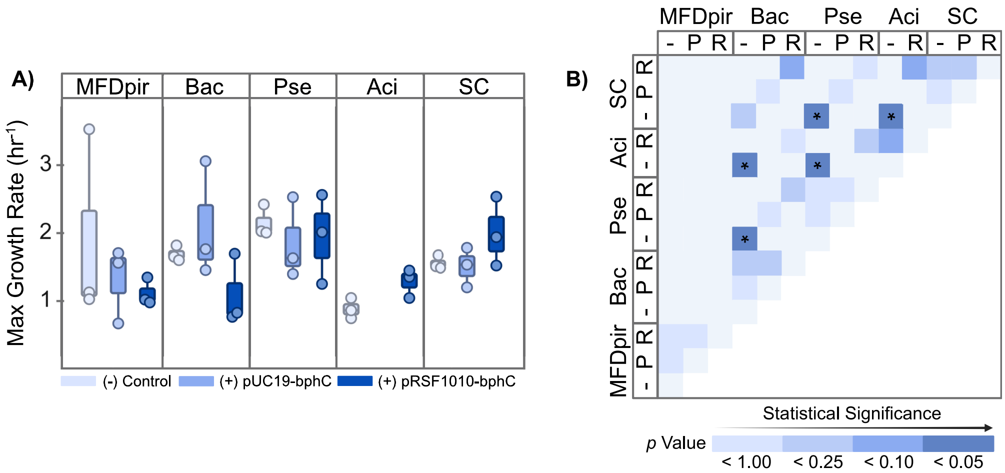

Figure 3. (A) Maximum growth rates (h^{-1}) determined from different recipient and plasmid combinations and a (B) heatmap showing p values based on a two-way ANOVA statistical analysis followed by a Tukey test from pairwise comparisons of maximum growth rates. p values below 0.05 are denoted as significant with an asterisk (*). Triplicate measurements are shown as dots, horizontal lines indicate the mean, and box plots indicate the standard deviation. Recipients include Bac, Pse, Aci, and SC. Nonengineered controls, as well as bacteria engineered with plasmids pUC19-bphC and pRSF1010-bphC are denoted as "-", P, and R, respectively.

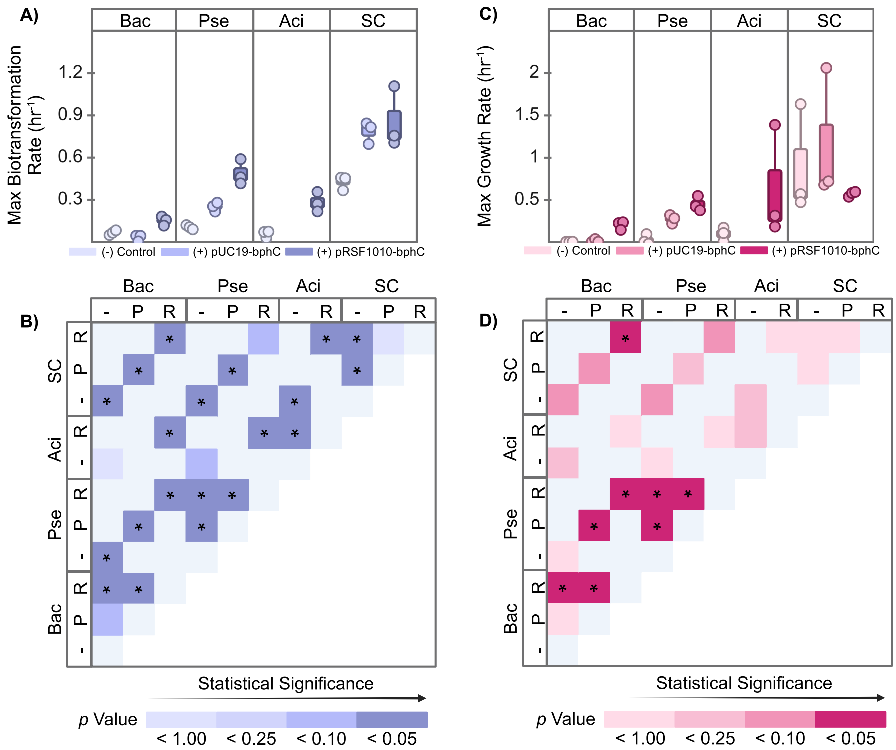

Figure 4. (A) Maximum biotransformation rates (h^{-1}) and (C) maximum growth rates (h^{-1}) determined from different recipient and plasmid combinations in M9 minimal media supplemented with a model PAH (2,3-dihydroxybiphenyl) and heatmaps showing p values based on a two-way ANOVA statistical analysis followed by a Tukey test from pairwise comparisons of (B) biotransformation rates and (D) growth rates. p values below 0.05 are denoted as significant with an asterisk (*). Triplicate measurements are shown as dots, horizontal lines indicate the mean, and box plots indicate the standard deviation. Recipients include Bac, Pse, Aci, and SC. Nonengineered controls, as well as bacteria engineered with plasmids pUC19-bphC and pRSF1010-bphC, are denoted as -, P, and R, respectively.

transconjugants were not significantly different (Figure 3B; $p > 0.10$), further corroborating 16S relative abundance and conjugation data in which *P. putida* recipients demonstrated the highest conjugation rate and abundance values.

Rates of PAH Biotransformation and Growth of Individual Strains Increased as a Result of Genetic Bioaugmentation

To investigate fitness impacts of introducing a catabolic dioxygenase enzyme to soil recipients via two different plasmids encoding *bphC*, we compared biotransformation rates of a model PAH (2,3-dihydroxybiphenyl) between engineered transconjugants and their nonengineered counterparts (Figure 4A). In addition to directly measuring the biotransformation rate of 2,3-dihydroxybiphenyl, we simultaneously measured bacterial growth to assess whether the bacteria could use a model PAH or metabolic byproducts as a carbon source for growth.

https://doi.org/10.1021/acsenvironau.4c00123
ACS Environ. Au 2025, 5, 241−252

We found that *P. putida* engineered with pRSF1010-bphC had maximum biotransformation rates that were significantly higher than nonengineered and pUC19-bphC engineered counterparts (Figure 4B; $p < 0.01$ and $p < 0.05$, respectively). Furthermore, *P. putida* engineered with pUC19-bphC transformed a model PAH at maximum rates significantly higher than those of nonengineered *P. putida* (Figure 4B; $p < 0.01$). Together, these findings are in agreement with growth data (Figure 4C) in which pUC19-bphC- and pRSF1010-bphC-engineered *P. putida* cultures had maximum growth rates significantly higher than nonengineered counterparts (Figure 4D; $p < 0.01$), indicating a positive fitness effect associated with plasmid-encoded *bphC* in the presence of a model PAH. For *B. subtilis*, we observed that *B. subtilis* engineered with pRSF1010-bphC had significantly higher maximum biotransformation and growth rates than their nonengineered and pUC19-bphC engineered counterparts (Figures 4B,D; $p < 0.05$ and $p < 0.01$, respectively). For *Acinetobacter* sp., the pRSF1010-bphC engineered bacteria had maximum biotransformation rates that were significantly higher than nonengineered *Acinetobacter* sp. (Figure 4B; $p < 0.01$), although maximum growth rates were not significantly different from one another (Figure 4D; $p > 0.10$).

In addition to comparing maximum biotransformation and growth rates between nonengineered and plasmid-engineered monocultures, we compared data across recipient bacteria. We found that *P. putida* engineered with either plasmid had higher maximum biotransformation and growth rates than all other monocultures engineered with the same plasmid backbones in minimal media supplemented with a model PAH. *P. putida* engineered with pUC19-bphC had significantly higher maximum biotransformation rates than those observed from *B. subtilis* engineered with pUC19-bphC (Figure 4B; $p < 0.01$). *P. putida* engineered with pRSF1010-bphC also had maximum biotransformation rates significantly higher than those demonstrated from both *B. subtilis* and *Acinetobacter* sp. engineered with pRSF1010-bphC (Figure 4B; $p < 0.01$ and $p < 0.05$, respectively). Together, these results were in agreement with the relative growth rates of these bacteria in the presence of a model PAH, as engineered *P. putida* had significantly higher growth rates than *B. subtilis* engineered with either plasmid derivative (Figure 4D; $p < 0.01$). Interestingly, maximum biotransformation rates observed from *B. subtilis* engineered with pRSF1010-bphC were significantly higher than those observed from *Acinetobacter* sp. engineered with pRSF1010-bphC (Figure 4B; $p < 0.05$), despite the fact that their growth rates were significantly similar (Figure 4D $p > 0.10$). Overall, most engineered strains demonstrated significantly higher biotransformation and growth rates when compared to their nonengineered counterparts. Thus, positive fitness effects were observed for plasmid-engineered soil bacteria in monocultures.

Higher Rates of Biotransformation and Growth were Observed in SCs When Compared to Monocultures

To demonstrate the impact of growing model soil bacteria in a community context on PAH biotransformation, we investigated the biotransformation and growth rates of soil bacteria grown in SCs and compared the results to those of monocultures. In contrast to trends observed from individual strains, the maximum growth rates from nonengineered SCs were not significantly different to those from pUC19-bphC and pRSF1010-bphC engineered communities (Figure 4D; $p > 0.10$). However, nonengineered SCs had significantly lower maximum biotransformation rates than pUC19-bphC and pRSF1010-bphC engineered counterparts (Figure 4B; $p < 0.01$ and $p < 0.05$, respectively). Moreover, maximum biotransformation rates of a model PAH were not significantly different between engineered SCs (Figure 4B; $p > 0.10$), indicating no difference in fitness effects between our plasmid backbones.

Interestingly, we observed that nonengineered communities demonstrated higher biotransformation and growth rates than nonengineered individual strains. The maximum biotransformation rates of a model PAH from nonengineered SCs were significantly higher than those observed from nonengineered *B. subtilis*, *P. putida*, and *Acinetobacter* sp. (Figure 4B; $p < 0.01$). These results were also consistent with growth rate data, as nonengineered SCs had maximum growth rates approximately one order of magnitude higher than *P. putida* and *Acinetobacter* sp. rates, and approximately five orders of magnitude higher than *B. subtilis* rates in media with PAH as the sole carbon source.

Maximum biotransformation rates of a model PAH from SCs engineered with pUC19-bphC were significantly higher than those observed from *B. subtilis* and *P. putida* engineered with pUC19-bphC (Figure 4B; $p < 0.01$). Furthermore, SCs engineered with pUC19-bphC had maximum growth rates approximately one and two orders of magnitude higher than those of *P. putida* and *B. subtilis* engineered with pUC19-bphC, respectively. Maximum biotransformation rates of a model PAH from SCs engineered with pRSF1010-bphC were significantly higher than those observed from *B. subtilis* and *Acinetobacter* sp. (Figure 4B; $p < 0.01$ and $p < 0.05$, respectively) and 76% ± 74 higher than those observed from *P. putida* engineered with the same plasmid. Overall, we found that *bphC*-engineered bacteria demonstrated higher biotransformation and growth rates when soil microbes were combined in SCs as opposed to individual cultures.

■ DISCUSSION

Conjugation and Growth Data Inform SC Assemblies

We incorporated donor, recipient, and transconjugant growth rates in conjugative transfer calculations to characterize and compare the conjugation of two different engineered plasmids with model soil bacteria. Additionally, we investigated how fitness effects of the plasmids influenced the SC assembly patterns. Our results show that the differences observed in conjugation rates between pUC19 and RSF1010 plasmids were not driven by differences in donor fitness, as growth rates of MFDpir engineered with either vector were not significantly different from nonengineered MFDpir growth rates. Additionally, differences in conjugation rates between pUC19 and RSF1010 vectors could not be explained by a conjugative mode of transfer, as both plasmids had the same *oriT* site recognized by the MFDpir donor RK2/RP4 conjugative machinery. We therefore focus on the effects of recipient fitness and discuss differences in maximum growth rates, host-specific proteins that interact with incoming plasmid DNA, and alternative routes of plasmid mobilization that may have contributed to observed differences in conjugative transfer rates.

Overall, conjugation rates were significantly associated with the relative abundances of the individual soil bacteria in SCs (Spearman $r = 0.886$ $p < 0.01$), indicating that conjugation rates and subsequent fitness impacts of plasmids influenced community assembly patterns. The *bphC* gene was delivered to recipients at significantly higher rates when using the low-copy RSF1010 backbone. The RSF1010 backbone, an Inc.-Q type plasmid, harbors its own complete replicon (*rep* genes) for initiating replication,[73] as well as proteins from the MOB_Q clade for mobilizing plasmids.[74] It is thought that this autonomous mode of plasmid replication and mobilization broadens the host range of RSF1010, as these activities do not rely on host-specific genes.[38] We observed different fitness impacts of the pRSF1010-bphC plasmid on different recipients. Specifically, maximum growth rates were lower for *B. subtilis* engineered with pRSF1010-bphC, indicating a negative fitness effect, which may explain the significant drop in the relative abundance of this transconjugant in SCs engineered with our pRSF1010-bphC plasmid. Furthermore, maximum growth rates of *P. putida* engineered with pRSF1010-bphC were significantly higher than those of *Acinetobacter* sp. engineered with the same plasmid, which explains the dominance of *P. putida* in SCs after conjugation with our RSF1010 derivative. Likewise, SCs engineered with pUC19-*bphC* were enriched with *B. subtilis*, the individual strain for which pUC19 conjugation and transconjugant growth rates were highest.

In contrast to RSF1010, pUC19 is a high-copy-number plasmid that can be maintained at up to 500 copies per cell.[39] High-copy-number plasmids have the potential to rapidly propagate in host cells; however, their conjugative transfer is often limited by the time required to (1) convert plasmid DNA into single-stranded DNA, (2) establish a mating pair formation between donor and recipient cells, and (3) mobilize DNA to new hosts.[40] An alternative route for mobilizing high-copy plasmid DNA may explain the higher observed conjugation rates of pUC19-bphC to *B. subtilis* compared to those of pRSF1010-bphC. A previous study showed that the same strain of *B. subtilis* used in our study has membrane-spanning nanotubes that can serve as conduits for exchanging plasmids,[75,76] particularly for small, high-copy plasmids.[77,78] In theory, high-copy number plasmids are coupled with elevated gene dosage effects using *B. subtilis* nanotubes for transfer, as plasmids may be freely exchanged between cytoplasmic spaces without the need to carefully synthesize and mobilize ssDNA.[79] Using these nanotubes, nonconjugative plasmids can be transferred from host bacteria to *B. subtilis* recipients via retrotransfer. To confirm this hypothesis, we performed conjugation experiments using pUC19 plasmid without an origin of transfer and observed plasmid transfer to *B. subtilis* from MFDpir (Table S6).

Although both *bphC* plasmids used in this study had the same origin of transfer, the pUC19 plasmid could not be conjugated to *P. putida* or *Acinetobacter* sp. at rates comparable with pRSF1010-bphC. Low transfer rates of high-copy pUC19 backbone, an Inc.P-type plasmid, to *P. putida* may be the result of a unique system encoded by a series of genes from *P. putida* (PTS^{Ntr}) that are known to inhibit the conjugative transfer of Inc.P plasmids from *E. coli* indirectly.[80] Still, some copies of pUC19-bphC were able to escape this DNA defense mechanism and replicate within *P. putida* with little effect on the growth of transconjugants. We were unable to conjugate pUC19-bphC to *Acinetobacter* sp. This is consistent with other studies that were unable to replicate pUC19 in *Acinetobacter* sp. post transformation,[81,82] although the exact reason is not well understood. Overall, we were able to capture fitness effects directly in our conjugative transfer rate calculations, and these effects were shown to predict SC assembly patterns.

Positive Growth and Biotransformation Effects Evident from Transconjugants

Although previous genetic bioaugmentation studies have investigated the horizontal gene transfer of catabolic genes to soil community members,[83−86] researchers often fail to characterize the functional activity of biodegradation genes in soil bacteria post conjugation, leading to unpredictable bioremediation results. In this study, we investigated the dioxygenase function of individual strains and SCs to assess whether engineered transconjugants could utilize plasmid-acquired *bphC* to degrade a model PAH at higher rates compared to their nonengineered counterparts. Overall, most soil microbes engineered with the *bphC* dioxygenase gene demonstrated significantly enhanced rates of biotransformation of a model PAH as compared to their nonengineered counterparts. Interestingly, nonengineered SCs were able to grow and degrade a model PAH at rates significantly higher than any of the individual nonengineered recipients. Together, these results suggest a synergistic effect between the presence of other community members and the bioaugmentation of *bphC*. Here, we elaborate on the effects of plasmid−host interactions, native dioxygenase activity, copy number, and bioavailability on the bioremediation of a model PAH.

Like *P. putida*,[87] *Acinetobacter* sp. recipients have been shown to efficiently transcribe plasmids from the MOB_Q family after acquiring plasmids in soil environments.[88] These findings corroborate our growth and biotransformation data, as *P. putida* and *Acinetobacter* sp. engineered with pRSF1010-bphC demonstrated significantly higher maximum growth and biotransformation rates than their nonengineered counterparts in minimal media, indicating positive fitness effects with respect to plasmid maintenance and *bphC* activity. Furthermore, *P. putida* transconjugants engineered with pRSF1010-bphC degraded a model PAH at maximum rates significantly higher than those of *Acinetobacter* sp. transconjugants. Our results suggest that this may not be a result of a difference in fitness with respect to growth, as *P. putida* and *Acinetobacter* sp. engineered with our RSF1010 derivative did not grow at maximum rates significantly different from one another. Instead, we suspect the difference in function between these transconjugants may have been due to the unusual metabolic diversity of *P. putida* isolated from soil matrices,[89] including more than 30 indigenous mono and dioxygenase enzymes.[90]

Individual soil bacteria engineered with pUC19-bphC had significantly lower growth and biotransformation rates than their pRSF1010-bphC engineered counterparts, suggesting negative fitness effects associated with maintaining the pUC19 backbone. Maintaining high copy numbers of pUC19 directs host DNA proteins away from growth-promoting metabolisms and may therefore impose a higher fitness cost on host organisms than low-copy RSF1010. Indeed, many studies have shown that directing resources away from host DNA replication and transcription toward maintaining high copy numbers of plasmid DNA prove deleterious with respect to growth and fitness of host cells.[40−42] Despite the high pUC19-bphC conjugation rate afforded by *B. subtilis* recipients, pRSF1010-bphC transconjugants showed significantly higher growth and biotransformation rates than nonengineered counterparts, while pUC19-bphC transconjugants did not. Still, *B. subtilis* engineered with pRSF1010-bphC showed

https://doi.org/10.1021/acsenvironau.4c00123
ACS Environ. Au 2025, 5, 241−252

significantly lower growth and biotransformation rates in comparison to other recipients engineered with the same plasmid. We believe the relatively low growth and biotransformation rates observed for engineered *B. subtilis* may be due to issues regarding the recognition and strength of the J23101 promoter directly upstream of *bphC*. Although the J23101 promoter works as a strong constitutive promoter in *E. coli*[91] and *P. putida*,[92] its strength is notably low in *B. subtilis*.[93] Future work should include testing different promoters upstream of functional genes to improve their activity in soil microbes.

Overall, SCs showed biotransformation rates significantly higher than those of monocultures, prompting further investigation into factors not related to plasmid fitness that may have contributed to the improved bioremediation of PAH residues. Amphiphilic molecules called biosurfactants collectively form micelles around hydrophobic residues, such as PAHs[94−96] and polychlorinated biphenyls[97,98] and promote the cellular uptake of these contaminants by reducing the surface tension across the aqueous and bacterial membrane interface. Biosurfactants from *Acinetobacter* sp. have been shown to advance PAH bioremediation when cultured with *P. putida*, as indigenous enzymes from *P. putida* participate in a biphenyl catabolic pathway.[99] Additionally, proteins translated from the chromosomal DNA of *P. putida* called phasins have been proposed as effective biosurfactants due to their amphiphilic characteristics as they coat hydrophobic granules and effectively increase their bioavailability.[100,101] The biosurfactant activity of either *Acinetobacter* sp. or *P. putida* could have increased the bioavailability of our model PAH for surrounding community members to utilize as a carbon source, as nonengineered communities showed maximum biotransformation rates significantly higher than species grown in monocultures. This is also true in the case of biotransformation rates across engineered cultures, with an additional increase in maximum biotransformation rates observed from *bphC*-engineered communities when compared to nonengineered communities. Together, the bioaugmentation of the *bphC* gene and the growth of soil bacteria in communities as opposed to monocultures were found to be synergistic with respect to increasing the bioremediation of a PAH.

CONCLUSIONS

In conclusion, we demonstrated that the fitness effects of plasmids used to deliver functional genes to soil bacteria impact growth rates, function, and community assembly patterns. We also highlighted the importance of pairing a functional assay with conjugation and growth data to assess the performance of engineered bacteria for PAH bioremediation. Additional analysis of the community composition after functional assays should be performed to study how the selective pressure imposed by a model PAH affects the fitness and assembly of transconjugants in a community context. Due to the remarkably high biodegradative capacity of nonengineered synthetic communities, future research should explore factors independent of plasmid fitness and consider how to incorporate biosurfactants with plasmid bioaugmentation designs for advancing PAH biodegradation. Finally, the fate and longevity of biodegradative plasmids, as well as the relative abundance of transconjugants, should be investigated over longer, more representative time periods in more complex environmental microbial communities.

ASSOCIATED CONTENT

Supporting Information

The Supporting Information is available free of charge at https://pubs.acs.org/doi/10.1021/acsenvironau.4c00123.

Tables describing plasmids, primer pairs, and cycling conditions; bacterial species; sequencing statistics; taxonomic classifications; plasmid maps and normalized absorbance data (PDF)

AUTHOR INFORMATION

Corresponding Author

Lauren B. Stadler − *Department of Civil and Environmental Engineering, Rice University, Houston, Texas 77006, United States*; orcid.org/0000-0001-7469-1981; Email: lauren.stadler@rice.edu

Author

Tessa M. Crosby − *Department of Civil and Environmental Engineering, Rice University, Houston, Texas 77006, United States*

Complete contact information is available at: https://pubs.acs.org/10.1021/acsenvironau.4c00123

Notes

The authors declare no competing financial interest.

ACKNOWLEDGMENTS

We thank Shyam Bhakta and the Bennett lab and Matthew Dysart and Prashant Kalvapalle and the Silberg lab at Rice University for donating the pRSF1010-bphC plasmid parts and bacterial species. We thank Bobby Tesoriero and Swetha Sridhar for their work in the original selection and characterization of the *bphC* gene. We thank Katherine Impelman and Katya Escalante for their contributions to this study. This work was funded by the National Science Foundation (Grant 2237052) and a Gulf Research Program Early Career Fellowship from the National Academies of Sciences, Engineering, and Medicine.

REFERENCES

(1) Barathi, S.; J, G.; Rathinasamy, G.; Sabapathi, N.; Aruljothi, K. N.; Lee, J.; Kandasamy, S. Recent Trends in Polycyclic Aromatic Hydrocarbons Pollution Distribution and Counteracting Bio-Remediation Strategies. *Chemosphere* **2023**, *337*, No. 139396.

(2) Meador, J. P. Bioaccumulation of PAHs in Marine Invertebrates. In *PAHs: An Ecotoxicological Perspective*; John Wiley & Sons, Ltd, 2003; pp 147−171. .

(3) Incardona, J. P.; Carls, M. G.; Teraoka, H.; Sloan, C. A.; Collier, T. K.; Scholz, N. L. Aryl Hydrocarbon Receptor−Independent Toxicity of Weathered Crude Oil during Fish Development. *Environ. Health Perspect.* **2005**, *113* (12), 1755−1762.

(4) Marquis, O.; Miaud, C.; Ficetola, G. F.; Bocher, A.; Mouchet, F.; Guittonneau, S.; Devaux, A. Variation in Genotoxic Stress Tolerance among Frog Populations Exposed to UV and Pollutant Gradients. *Aquat. Toxicol.* **2009**, *95* (2), 152−161.

(5) Labib, S.; Yauk, C.; Williams, A.; Arlt, V. M.; Phillips, D. H.; White, P. A.; Halappanavar, S. Subchronic Oral Exposure to Benzo(a)Pyrene Leads to Distinct Transcriptomic Changes in the Lungs That Are Related to Carcinogenesis. *Toxicol. Sci.* **2012**, *129* (1), 213−224.

(6) Martineau, D.; Lemberger, K.; Dallaire, A.; Labelle, P.; Lipscomb, T. P.; Michel, P.; Mikaelian, I. Cancer in Wildlife, a

Case Study: Beluga from the St. Lawrence Estuary, Québec, Canada. *Environ. Health Perspect.* **2002**, *110* (3), 285−292.

(7) Etkin, D. S.; Welch, J. Oil spill intelligence report international oil spill database: trends in oil spill volumes and frequency1. *Int. Oil Spill Conf. Proc.* **1997**, 949.

(8) Ince, M.; Ince, O. K.; Ondrasek, G. *Biochemical Toxicology: Heavy Metals and Nanomaterials;*; BoD − Books on Demand, 2020.

(9) Reyes, G. G. Genotoxicity by Pahs In Shrimp (Litopenaeus Vannamei) and Its Impact on The Aquaculture of Two Coastal Ecosystems of The Gulf of California, Mexico, *Eur. J. Agric. Food Sci.* **2020**, *2*. 4, .

(10) Tiku, D. Toxicity of Crude Oil and Diesel Fuel to Some Gram Positive and Gram Negative Bacterial. *Imp. J. Interdiscip. Res. IJIR* **2016**, *2*, 273.

(11) Nwadibe, E. C.; Aniebonam, E. E.; Jude, O. U. EFFECT OF CRUDE OIL POLLUTION ON SOIL AND AQUATIC BACTERIA AND FUNGI. *J. Exp. Biol. Agric. Sci.* **2020**, *8*, 176−184.

(12) Heipieper, H. J.; Cornelissen, S.; Pepi, M. Surface Properties and Cellular Energetics of Bacteria in Response to the Presence of Hydrocarbons. In *Handbook of Hydrocarbon and Lipid Microbiology*; Timmis, K. N., Ed.; Springer: Berlin, Heidelberg, 2010; pp 1615−1624. .

(13) Adedokun, O.; Ataga, A. Effects of Amendments and Bioaugumentation of Soil Polluted with Crude Oil, Automotive Gasoline Oil, and Spent Engine Oil on the Growth of Cowpea (Vigna Ungiculata L. Walp). *Sci. Res. Essay* **2007**, *2*, 147−149.

(14) Geng, S.; Cao, W.; Yuan, J.; Wang, Y.; Guo, Y.; Ding, A.; Zhu, Y.; Dou, J. Microbial Diversity and Co-Occurrence Patterns in Deep Soils Contaminated by Polycyclic Aromatic Hydrocarbons (PAHs). *Ecotoxicol. Environ. Saf.* **2020**, *203*, No. 110931.

(15) Urakawa, H.; Garcia, J. C.; Barreto, P. D.; Molina, G. A.; Barreto, J. C. A Sensitive Crude Oil Bioassay Indicates That Oil Spills Potentially Induce a Change of Major Nitrifying Prokaryotes from the Archaea to the Bacteria. *Environ. Pollut.* **2012**, *164*, 42−45.

(16) Duarte, M.; Nielsen, A.; Camarinha-Silva, A.; Vilchez-Vargas, R.; Bruls, T.; Wos-Oxley, M. L.; Jauregui, R.; Pieper, D. H. Functional Soil Metagenomics: Elucidation of Polycyclic Aromatic Hydrocarbon Degradation Potential Following 12 Years of in Situ Bioremediation. *Environ. Microbiol.* **2017**, *19* (8), 2992−3011.

(17) Innemanová, P.; Filipová, A.; Michalíková, K.; Wimmerová, L.; Cajthaml, T. Bioaugmentation of PAH-Contaminated Soils: A Novel Procedure for Introduction of Bacterial Degraders into Contaminated Soil. *Ecol. Eng.* **2018**, *118*, 93−96.

(18) Zhang, C.; Wu, D.; Ren, H. Bioremediation of Oil Contaminated Soil Using Agricultural Wastes via Microbial Consortium. *Sci. Rep.* **2020**, *10* (1), 9188.

(19) Rezek, J.; in der Wiesche, C.; Mackova, M.; Zadrazil, F.; Macek, T. The Effect of Ryegrass (*Lolium Perenne*) on Decrease of PAH Content in Long Term Contaminated Soil. *Chemosphere* **2008**, *70* (9), 1603−1608.

(20) Dhar, K.; Panneerselvan, L.; Venkateswarlu, K.; Megharaj, M. Efficient Bioremediation of PAHs-Contaminated Soils by a Methylotrophic Enrichment Culture. *Biodegradation* **2022**, *33* (6), 575−591.

(21) Mandree, P.; Masika, W.; Naicker, J.; Moonsamy, G.; Ramchuran, S.; Lalloo, R. Bioremediation of Polycyclic Aromatic Hydrocarbons from Industry Contaminated Soil Using Indigenous Bacillus Spp. *Processes* **2021**, *9* (9), 1606.

(22) Tomar, R. S.; Rai-Kalal, P.; Jajoo, A. Impact of Polycyclic Aromatic Hydrocarbons on Photosynthetic and Biochemical Functions and Its Bioremediation by *Chlorella Vulgaris*. *Algal Res.* **2022**, *67*, No. 102815.

(23) Lu, C.; Hong, Y.; Liu, J.; Gao, Y.; Ma, Z.; Yang, B.; Ling, W.; Waigi, M. G. A PAH-Degrading Bacterial Community Enriched with Contaminated Agricultural Soil and Its Utility for Microbial Bioremediation. *Environ. Pollut.* **2019**, *251*, 773−782.

(24) Radwan, S. s.; Sorkhoh, N. a.; El-Nemr, I. m.; El-Desouky, A. f. A Feasibility Study on Seeding as a Bioremediation Practice for the Oily Kuwaiti Desert. *J. Appl. Microbiol.* **1997**, *83* (3), 353−358.

(25) Simarro, R.; González, N.; Bautista, L. F.; Molina, M. C. Assessment of the Efficiency of *in Situ* Bioremediation Techniques in a Creosote Polluted Soil: Change in Bacterial Community. *J. Hazard. Mater.* **2013**, *262*, 158−167.

(26) Ma, Y.; Wang, L.; Shao, Z. Pseudomonas, the Dominant Polycyclic Aromatic Hydrocarbon-Degrading Bacteria Isolated from Antarctic Soils and the Role of Large Plasmids in Horizontal Gene Transfer. *Environ. Microbiol.* **2006**, *8* (3), 455−465.

(27) Ginn, T. R.; Un Jan Contreras, S.; Gardner, C. M.; Falcon, G.; Maguire, L. Horizontal Gene Transfer in Soils: Column Experiments in Transgene Transport and Uptake. *SAO Astrophys. Data System.* **2023**, *2023*, H53C−01.

(28) Zhao, S.; Rogers, M. J.; Ding, C.; Xu, G.; He, J. Interspecies Mobility of Organohalide Respiration Gene Clusters Enables Genetic Bioaugmentation. *Environ. Sci. Technol.* **2024**, *58* (9), 4214−4225.

(29) Ogunseitan, O. A.; Tedford, E. T.; Pacia, D.; Sirotkin, K. M.; Sayler, G. S. Distribution of Plasmids in Groundwater Bacteria. *J. Ind. Microbiol.* **1987**, *1* (5), 311−317.

(30) Khatoon, K.; Malik, A. Screening of Polycyclic Aromatic Hydrocarbon Degrading Bacterial Isolates from Oil Refinery Wastewater and Detection of Conjugative Plasmids in Polycyclic Aromatic Hydrocarbon Tolerant and Multi-Metal Resistant Bacteria. *Heliyon* **2019**, *5* (10), 20219939141.

(31) Liu, S. Ecology and Evolution of Microbial Populations for Bioremediation. *Trends Biotechnol.* **1993**, *11* (8), 344−352.

(32) Martinez, J. L. The Role of Natural Environments in the Evolution of Resistance Traits in Pathogenic Bacteria. *Proc. R. Soc. B Biol. Sci.* **2009**, *276* (1667), 2521−2530.

(33) Ikuma, K.; Gunsch, C. K. Genetic Bioaugmentation as an Effective Method for in Situ Bioremediation: Functionality of Catabolic Plasmids Following Conjugal Transfers. *Bioengineered* **2012**, *3* (4), 236−241.

(34) Ifediegwu, M. C.; Uba, B. O.; Awari, V. G.; Okongwu, D. J. Biodegradation of Bonny Light Crude Oil by Plasmid and Non-Plasmid Borne Soil Bacterial Strains Using Biostimulation and Bioaugmentation Techniques. *Sci. World J.* **2024**, *19* (1), 178−188.

(35) Varner, P. M.; Allemann, M. N.; Michener, J. K.; Gunsch, C. K. The Effect of Bacterial Growth Strategies on Plasmid Transfer and Naphthalene Degradation for Bioremediation. *Environ. Technol. Innov.* **2022**, *28*, No. 102910.

(36) Frey, J.; Bagdasarian, M. M.; Bagdasarian, M. Replication and Copy Number Control of the Broad-Host-Range Plasmid RSF1010. *Gene* **1992**, *113* (1), 101−106.

(37) Meyer, R. Mapping Type IV Secretion Signals on the Primase Encoded by the Broad-Host-Range Plasmid R1162 (RSF1010). *J. Bacteriol.* **2015**, *197* (20), 3245−3254.

(38) Scholz, P.; Haring, V.; Wittmann-Liebold, B.; Ashman, K.; Bagdasarian, M.; Scherzinger, E. Complete Nucleotide Sequence and Gene Organization of the Broad-Host-Range Plasmid RSF1010. *Gene* **1989**, *75* (2), 271−288.

(39) Lin-Chao, S.; Chen, W.-T.; Wong, T.-T. High Copy Number of the pUC Plasmid Results from a Rom/Rop-Suppressible Point Mutation in RNA II. *Mol. Microbiol.* **1992**, *6* (22), 3385−3393.

(40) Watve, M. M.; Dahanukar, N.; Watve, M. G. Sociobiological Control of Plasmid Copy Number in Bacteria. *PLoS One* **2010**, *5* (2), No. e9328.

(41) Münch, K.; Münch, R.; Biedendieck, R.; Jahn, D.; Müller, J. Evolutionary Model for the Unequal Segregation of High Copy Plasmids. *PLOS Comput. Biol.* **2019**, *15* (3), No. e1006724.

(42) San Millan, A.; MacLean, R. C. Fitness Costs of Plasmids: A Limit to Plasmid Transmission. *Microbiol. Spectr.* **2017**, *5* (5), 10.

(43) Kaur, R.; Gupta, S.; Tripathi, V.; Chauhan, A.; Parashar, D.; Shankar, P.; Kashyap, V. Microbiome Based Approaches for the Degradation of Polycyclic Aromatic Hydrocarbons (PAHs): A Current Perception. *Chemosphere* **2023**, *341*, No. 139951.

(44) Miao, L.-L.; Qu, J.; Liu, Z.-P. Hydroxylation at Multiple Positions Initiated the Biodegradation of Indeno[1,2,3-Cd]Pyrene in Rhodococcus Aetherivorans IcdP1. *Front. Microbiol.* **2020**, *11*, No. 568381.

(45) Wu, Y.; Xu, Y.; Zhou, N. A Newly Defined Dioxygenase System from Mycobacterium Vanbaalenii PYR-1 Endowed with an Enhanced Activity of Dihydroxylation of High-Molecular-Weight Polyaromatic Hydrocarbons. *Front. Environ. Sci. Eng.* **2020**, *14* (1), 14.

(46) Hayase, N.; Taira, K.; Furukawa, K. Pseudomonas Putida KF715 bphABCD Operon Encoding Biphenyl and Polychlorinated Biphenyl Degradation: Cloning, Analysis, and Expression in Soil Bacteria. *J. Bacteriol.* **1990**, *172* (2), 1160−1164.

(47) Kosono, S.; Maeda, M.; Fuji, F.; Arai, H.; Kudo, T. Three of the Seven bphC Genes of Rhodococcus Erythropolis TA421, Isolated from a Termite Ecosystem, Are Located on an Indigenous Plasmid Associated with Biphenyl Degradation. *Appl. Environ. Microbiol.* **1997**, *63* (8), 3282−3285.

(48) Hirose, J.; Fujihara, H.; Watanabe, T.; Kimura, N.; Suenaga, H.; Futagami, T.; Goto, M.; Suyama, A.; Furukawa, K. Biphenyl/PCB Degrading Bph Genes of Ten Bacterial Strains Isolated from Biphenyl-Contaminated Soil in Kitakyushu, Japan: Comparative and Dynamic Features as Integrative Conjugative Elements (ICEs). *Genes* **2019**, *10* (5), 404.

(49) Furukawa, K.; Hirose, J.; Suyama, A.; Zaiki, T.; Hayashida, S. Gene Components Responsible for Discrete Substrate Specificity in the Metabolism of Biphenyl (Bph Operon) and Toluene (Tod Operon). *J. Bacteriol.* **1993**, *175* (16), 5224−5232.

(50) Jia, Y.; Wang, J.; Ren, C.; Nahurira, R.; Khokhar, I.; Wang, J.; Fan, S.; Yan, Y. Identification and Characterization of a Meta-Cleavage Product Hydrolase Involved in Biphenyl Degradation from Arthrobacter Sp. YC-RL1. *Appl. Microbiol. Biotechnol.* **2019**, *103* (16), 6825−6836.

(51) Riegert, U.; Heiss, G.; Fischer, P.; Stolz, A. Distal Cleavage of 3-Chlorocatechol by an Extradiol Dioxygenase to 3-Chloro-2-Hydroxymuconic Semialdehyde. *J. Bacteriol.* **1998**, *180* (11), 2849−2853.

(52) Ding, Y.; Ren, H.; Hao, X.; Zhang, R.; Hao, J.; Liu, J.; Pan, H.; Wang, Y. Enhanced Phytoremediation of PCBs-Contaminated Soil by Co-Expressing *tfdB* and *bphC* in *Arabidopsis* Aiding in Metabolism and Improving Toxicity Tolerance. *Environ. Exp. Bot.* **2024**, *217*, No. 105548.

(53) Novakova, M.; Mackova, M.; Chrastilova, Z.; Viktorova, J.; Szekeres, M.; Demnerova, K.; Macek, T. Cloning the Bacterial bphC Gene into Nicotiana Tabacum to Improve the Efficiency of PCB Phytoremediation. *Biotechnol. Bioeng.* **2009**, *102* (1), 29−37.

(54) Ferrières, L.; Hémery, G.; Nham, T.; Guérout, A.-M.; Mazel, D.; Beloin, C.; Ghigo, J.-M. Silent Mischief: Bacteriophage Mu Insertions Contaminate Products of Escherichia Coli Random Mutagenesis Performed Using Suicidal Transposon Delivery Plasmids Mobilized by Broad-Host-Range RP4 Conjugative Machinery. *J. Bacteriol.* **2010**, *192* (24), 6418−6427.

(55) Huisman, J. S.; Benz, F.; Duxbury, S. J. N.; de Visser, J. A. G. M.; Hall, A. R.; Fischer, E. A. J.; Bonhoeffer, S. Estimating Plasmid Conjugation Rates: A New Computational Tool and a Critical Comparison of Methods. *Plasmid* **2022**, *121*, No. 102627.

(56) Wiser, M. J.; Lenski, R. E. A Comparison of Methods to Measure Fitness in Escherichia Coli. *PLoS One* **2015**, *10* (5), No. e0126210.

(57) Frey, P. M.; Baer, J.; Bergada-Pijuan, J.; Lawless, C.; Bühler, P. K.; Kouyos, R. D.; Lemon, K. P.; Zinkernagel, A. S.; Brugger, S. D. Quantifying Variation in Bacterial Reproductive Fitness: A High-Throughput Method. *mSystems* **2021**, *6* (1), 10.

(58) Hall, B. G.; Acar, H.; Nandipati, A.; Barlow, M. Growth Rates Made Easy. *Mol. Biol. Evol.* **2014**, *31* (1), 232−238.

(59) Wetmore, K. M.; Price, M. N.; Waters, R. J.; Lamson, J. S.; He, J.; Hoover, C. A.; Blow, M. J.; Bristow, J.; Butland, G.; Arkin, A. P.; Deutschbauer, A. Rapid Quantification of Mutant Fitness in Diverse Bacteria by Sequencing Randomly Bar-Coded Transposons. *mBio* **2015**, *6* (3), 10.

(60) Fink, J. W.; Manhart, M. Quantifying Microbial Fitness in High-Throughput Experiments. *bioRxiv* **2024**, 2024.08.20.608874.

(61) Bolyen, E.; Rideout, J. R.; Dillon, M. R.; Bokulich, N. A.; Abnet, C. C.; Al-Ghalith, G. A.; Alexander, H.; Alm, E. J.; Arumugam, M.; Asnicar, F.; Bai, Y.; Bisanz, J. E.; Bittinger, K.; Brejnrod, A.; Brislawn, C. J.; Brown, C. T.; Callahan, B. J.; Caraballo-Rodríguez, A. M.; Chase, J.; Cope, E. K.; Da Silva, R.; Diener, C.; Dorrestein, P. C.; Douglas, G. M.; Durall, D. M.; Duvallet, C.; Edwardson, C. F.; Ernst, M.; Estaki, M.; Fouquier, J.; Gauglitz, J. M.; Gibbons, S. M.; Gibson, D. L.; Gonzalez, A.; Gorlick, K.; Guo, J.; Hillmann, B.; Holmes, S.; Holste, H.; Huttenhower, C.; Huttley, G. A.; Janssen, S.; Jarmusch, A. K.; Jiang, L.; Kaehler, B. D.; Kang, K. B.; Keefe, C. R.; Keim, P.; Kelley, S. T.; Knights, D.; Koester, I.; Kosciolek, T.; Kreps, J.; Langille, M. G. I.; Lee, J.; Ley, R.; Liu, Y.-X.; Loftfield, E.; Lozupone, C.; Maher, M.; Marotz, C.; Martin, B. D.; McDonald, D.; McIver, L. J.; Melnik, A. V.; Metcalf, J. L.; Morgan, S. C.; Morton, J. T.; Naimey, A. T.; Navas-Molina, J. A.; Nothias, L. F.; Orchanian, S. B.; Pearson, T.; Peoples, S. L.; Petras, D.; Preuss, M. L.; Pruesse, E.; Rasmussen, L. B.; Rivers, A.; Robeson, M. S.; Rosenthal, P.; Segata, N.; Shaffer, M.; Shiffer, A.; Sinha, R.; Song, S. J.; Spear, J. R.; Swafford, A. D.; Thompson, L. R.; Torres, P. J.; Trinh, P.; Tripathi, A.; Turnbaugh, P. J.; Ul-Hasan, S.; van der Hooft, J. J. J.; Vargas, F.; Vázquez-Baeza, Y.; Vogtmann, E.; von Hippel, M.; Walters, W.; Wan, Y.; Wang, M.; Warren, J.; Weber, K. C.; Williamson, C. H. D.; Willis, A. D.; Xu, Z. Z.; Zaneveld, J. R.; Zhang, Y.; Zhu, Q.; Knight, R.; Caporaso, J. G. Author Correction: Reproducible, Interactive, Scalable and Extensible Microbiome Data Science Using QIIME 2. *Nat. Biotechnol.* **2019**, *37* (9), 1091−1091.

(62) Estaki, M.; Jiang, L.; Bokulich, N. A.; McDonald, D.; González, A.; Kosciolek, T.; Martino, C.; Zhu, Q.; Birmingham, A.; Vázquez-Baeza, Y.; Dillon, M. R.; Bolyen, E.; Caporaso, J. G.; Knight, R. QIIME 2 Enables Comprehensive End-to-End Analysis of Diverse Microbiome Data and Comparative Studies with Publicly Available Data. *Curr. Protoc. Bioinforma.* **2020**, *70* (1), No. e100.

(63) Caruso, V.; Song, X.; Asquith, M.; Karstens, L. Performance of Microbiome Sequence Inference Methods in Environments with Varying Biomass. *mSystems* **2019**, *4* (1), 10.

(64) Callahan, B. J.; McMurdie, P. J.; Rosen, M. J.; Han, A. W.; Johnson, A. J. A.; Holmes, S. P. DADA2: High-Resolution Sample Inference from Illumina Amplicon Data. *Nat. Methods* **2016**, *13* (7), 581−583.

(65) Furukawa, K.; Miyazaki, T. Cloning of a Gene Cluster Encoding Biphenyl and Chlorobiphenyl Degradation in Pseudomonas Pseudoalcaligenes. *J. Bacteriol.* **1986**, *166* (2), 392−398.

(66) Vaillancourt, F. H.; Labbé, G.; Drouin, N. M.; Fortin, P. D.; Eltis, L. D. The Mechanism-Based Inactivation of 2,3-Dihydroxybiphenyl 1,2-Dioxygenase by Catecholic Substrates *. *J. Biol. Chem.* **2002**, *277* (3), 2019−2027.

(67) Catelani, D.; Colombi, A.; Sorlini, C.; Treccani, V. Metabolism of Biphenyl. 2-Hydroxy-6-Oxo-6-Phenylhexa-2,4-Dienoate: The Meta-Cleavage Product from 2,3-Dihydroxybiphenyl by Pseudomonas Putida. *Biochem. J.* **1973**, *134* (4), 1063−1066.

(68) Sadiq, F. A.; De Reu, K.; Burmølle, M.; Maes, S.; Heyndrickx, M. Synergistic Interactions in Multispecies Biofilm Combinations of Bacterial Isolates Recovered from Diverse Food Processing Industries. *Front. Microbiol.* **2023**, *14*, 1159434.

(69) Sadiq, F. A.; De Reu, K.; Steenackers, H.; Van de Walle, A.; Burmølle, M.; Heyndrickx, M. Dynamic Social Interactions and Keystone Species Shape the Diversity and Stability of Mixed-Species Biofilms − an Example from Dairy Isolates. *ISME Commun.* **2023**, *3* (1), 1−12.

(70) Slinker, B. K. The Statistics of Synergism. *J. Mol. Cell. Cardiol.* **1998**, *30* (4), 723−731.

(71) Mangiafico, S. *R Companion: Contrasts in Linear Models*. Post-hoc Contrasts in Models. https://rcompanion.org/rcompanion/h_01.html (accessed 2024−10−22).

(72) Simonsen, L.; Gordon, D. M.; Stewart, F. M.; Levin, B. R. Estimating the Rate of Plasmid Transfer: An End-Point Method. *Microbiology* **1990**, *136* (11), 2319−2325.

(73) Scherzinger, E.; Haring, V.; Lurz, R.; Otto, S. Plasmid RSF1010 DNA Replication in Vitro Promoted by Purified RSF1010 RepA, RepB and RepC Proteins. *Nucleic Acids Res.* **1991**, *19* (6), 1203−1211.

(74) Derbyshire, K. M.; Hatfull, G.; Willetts, N. Mobilization of the Non-Conjugative Plasmid RSF1010: A Genetic and DNA Sequence Analysis of the Mobilization Region. *Mol. Gen. Genet. MGG* **1987**, *206* (1), 161−168.
(75) Dubey, G. P.; Ben-Yehuda, S. Intercellular Nanotubes Mediate Bacterial Communication. *Cell* **2011**, *144* (4), 590−600.
(76) Ficht, T. A. Bacterial Exchange via Nanotubes: Lessons Learned from the History of Molecular Biology. *Front. Microbiol.* **2011**, *2*, 179.
(77) Morawska, L. P.; Kuipers, O. P. Cell-to-Cell Non-Conjugative Plasmid Transfer between Bacillus Subtilis and Lactic Acid Bacteria. *Microb. Biotechnol.* **2023**, *16* (4), 784−798.
(78) Zhao, X.; Xu, J.; Tan, M.; Zhen, J.; Shu, W.; Yang, S.; Ma, Y.; Zheng, H.; Song, H. High Copy Number and Highly Stable Escherichia Coli−Bacillus Subtilis Shuttle Plasmids Based on pWB980. *Microb. Cell Factories* **2020**, *19* (1), 25.
(79) Dubey, G. P.; Malli Mohan, G. B.; Dubrovsky, A.; Amen, T.; Tsipshtein, S.; Rouvinski, A.; Rosenberg, A.; Kaganovich, D.; Sherman, E.; Medalia, O.; Ben-Yehuda, S. Architecture and Characteristics of Bacterial Nanotubes. *Dev. Cell* **2016**, *36* (4), 453−461.
(80) Inoue, K.; Miyazaki, R.; Ohtsubo, Y.; Nagata, Y.; Tsuda, M. Inhibitory Effect of Pseudomonas Putida Nitrogen-Related Phosphotransferase System on Conjugative Transfer of IncP-9 Plasmid from Escherichia Coli. *FEMS Microbiol. Lett.* **2013**, *345* (2), 102−109.
(81) Cosper, N. J.; Collier, L. S.; Clark, T. J.; Scott, R. A.; Neidle, E. L. Mutations in catB, the Gene Encoding Muconate Cycloisomerase, Activate Transcription of the Distalben Genes and Contribute to a Complex Regulatory Circuit in Acinetobacter Sp. Strain ADP1. *J. Bacteriol.* **2000**, *182* (24), 7044−7052.
(82) Hare, J. M.; Perkins, S. N.; Gregg-Jolly, L. A. A Constitutively Expressed, Truncated umuDC Operon Regulates the recA-Dependent DNA Damage Induction of a Gene in Acinetobacter Baylyi Strain ADP1. *Appl. Environ. Microbiol.* **2006**, *72* (6), 4036−4043.
(83) Dejonghe, W.; Goris, J.; El Fantroussi, S.; Höfte, M.; De Vos, P.; Verstraete, W.; Top, E. M. Effect of Dissemination of 2,4-Dichlorophenoxyacetic Acid (2,4-D) Degradation Plasmids on 2,4-D Degradation and on Bacterial Community Structure in Two Different Soil Horizons. *Appl. Environ. Microbiol.* **2000**, *66* (8), 3297−3304.
(84) Inoue, D.; Yamazaki, Y.; Tsutsui, H.; Sei, K.; Soda, S.; Fujita, M.; Ike, M. Impacts of Gene Bioaugmentation with pJP4-Harboring Bacteria of 2,4-D-Contaminated Soil Slurry on the Indigenous Microbial Community. *Biodegradation* **2012**, *23* (2), 263−276.
(85) Newby, D. T.; Gentry, T. J.; Pepper, I. L. Comparison of 2,4-Dichlorophenoxyacetic Acid Degradation and Plasmid Transfer in Soil Resulting from Bioaugmentation with Two Different pJP4 Donors. *Appl. Environ. Microbiol.* **2000**, *66* (8), 3399−3407.
(86) Newby, D. T.; Pepper, I. L. Dispersal of Plasmid pJP4 in Unsaturated and Saturated 2,4-Dichlorophenoxyacetic Acid Contaminated Soil. *FEMS Microbiol. Ecol.* **2002**, *39* (2), 157−164.
(87) Romaniuk, K.; Styczynski, M.; Decewicz, P.; Buraczewska, O.; Uhrynowski, W.; Fondi, M.; Wolosiewicz, M.; Szuplewska, M.; Dziewit, L. Diversity and Horizontal Transfer of Antarctic Pseudomonas Spp. Plasmids. *Genes* **2019**, *10* (11), 850.
(88) Salto, I. P.; Torres Tejerizo, G.; Wibberg, D.; Pühler, A.; Schlüter, A.; Pistorio, M. Comparative Genomic Analysis of Acinetobacter Spp. Plasmids Originating from Clinical Settings and Environmental Habitats. *Sci. Rep.* **2018**, *8* (1), 7783.
(89) Shrestha, S.; Awasthi, D.; Chen, Y.; Gin, J.; Petzold, C. J.; Adams, P. D.; Simmons, B. A.; Singer, S. W. Simultaneous Carbon Catabolite Repression Governs Sugar and Aromatic Co-Utilization in Pseudomonas Putida M2. *Appl. Environ. Microbiol.* **2023**, *89* (10), e00852−23.
(90) Dos Santos, V. A. P. M.; Heim, S.; Moore, E. R. B.; Strätz, M.; Timmis, K. N. Insights into the Genomic Basis of Niche Specificity of Pseudomonas Putida KT2440. *Environ. Microbiol.* **2004**, *6* (12), 1264−1286.
(91) Davis, J. H.; Rubin, A. J.; Sauer, R. T. Design, Construction and Characterization of a Set of Insulated Bacterial Promoters. *Nucleic Acids Res.* **2011**, *39* (3), 1131−1141.
(92) Thompson, M. G.; Costello, Z.; Hummel, N. F. C.; Cruz-Morales, P.; Blake-Hedges, J. M.; Krishna, R. N.; Skyrud, W.; Pearson, A. N.; Incha, M. R.; Shih, P. M.; Garcia-Martin, H.; Keasling, J. D. Robust Characterization of Two Distinct Glutarate Sensing Transcription Factors of Pseudomonas Putida L-Lysine Metabolism. *ACS Synth. Biol.* **2019**, *8* (10), 2385−2396.
(93) Radeck, J.; Kraft, K.; Bartels, J.; Cikovic, T.; Dürr, F.; Emenegger, J.; Kelterborn, S.; Sauer, C.; Fritz, G.; Gebhard, S.; Mascher, T. The Bacillus BioBrick Box: Generation and Evaluation of Essential Genetic Building Blocks for Standardized Work with Bacillus Subtilis. *J. Biol. Eng.* **2013**, *7* (1), 29.
(94) Bezza, F. A.; Nkhalambayausi Chirwa, E. M. Biosurfactant-Enhanced Bioremediation of Aged Polycyclic Aromatic Hydrocarbons (PAHs) in Creosote Contaminated Soil. *Chemosphere* **2016**, *144*, 635−644.
(95) Cameotra, S. S.; Makkar, R. S. Biosurfactant-enhanced bioremediation of hydrophobic pollutants. *Pure Appl. Chem.* **2010**, *82* (1), 97−116.
(96) Zang, T.; Wu, H.; Yan, B.; Zhang, Y.; Wei, C. Enhancement of PAHs Biodegradation in Biosurfactant/Phenol System by Increasing the Bioavailability of PAHs. *Chemosphere* **2021**, *266*, No. 128941.
(97) Sandhu, M.; Paul, A. T.; Proćków, J.; de la Lastra, J. M. P.; Jha, P. N. PCB-77 Biodegradation Potential of Biosurfactant Producing Bacterial Isolates Recovered from Contaminated Soil. *Front. Microbiol.* **2022**, *13*. .
(98) Sifour, M.; H. Al-Jila, M.; M. Aziz, G. Emulsification Properties of Biosurfactant Produced from Pseudomonas Aeruginosa RB 28. *Pak. J. Biol. Sci.* **2007**, *10* (8), 1331−1335.
(99) Zhou, H.; Huang, X.; Liang, Y.; Li, Y.; Xie, Q.; Zhang, C.; You, S. Enhanced Bioremediation of Hydraulic Fracturing Flowback and Produced Water Using an Indigenous Biosurfactant-Producing Bacteria *Acinetobacter* Sp. Y2. *Chem. Eng. J.* **2020**, *397*, No. 125348.
(100) Mato, A.; Tarazona, N. A.; Hidalgo, A.; Cruz, A.; Jiménez, M.; Pérez-Gil, J.; Prieto, M. A. Interfacial Activity of Phasin PhaF from Pseudomonas Putida KT2440 at Hydrophobic−Hydrophilic Biointerfaces. *Langmuir* **2019**, *35* (3), 678−686.
(101) Ortega Ramírez, C. A.; Ching, T.; Yoza, B.; Li, Q. X. Glycerol-Assisted Degradation of Dibenzothiophene by *Paraburkholderia* Sp. C3 Is Associated with Polyhydroxyalkanoate Granulation. *Chemosphere* **2022**, *291*, No. 133054.

https://doi.org/10.1021/acsenvironau.4c00123
ACS Environ. Au 2025, 5, 241−252